



Synthesis, performance, and nonlinear modeling of modified nano-sized magnetite for removal of Cr(VI) from aqueous solutions

Ali Akbar Babaei^{a,b}, Zeynab Baboli^b, Nemat Jaafarzadeh^{a,b}, Gholamreza Goudarzi^{a,b}, Mehdi Bahrami^c, Mehdi Ahmadi^{a,b,*}

^a*Environmental Technologies Research Center, Ahvaz Jundishapur University of Medical Sciences, Ahvaz, Iran
Tel. +98 611 3738269; Fax: +98 611 3738282; email: Ahmadi241@yahoo.com*

^b*Department of Environmental Health Engineering, School of Public Health, Ahvaz Jundishapur University of Medical Sciences, Ahvaz, Iran*

^c*School of Water Sciences Engineering, Shahid Chamran University, Ahvaz, Iran*

Received 9 May 2013; Accepted 8 September 2013

ABSTRACT

Contamination of water bodies with toxic and non-biodegradable heavy metals is a serious environmental problem. Chromium is a very important contaminant in soil, industrial waste, groundwater, and surface water sources. This study was conducted to assess hexavalent chromium (Cr(VI)) adsorption onto modified magnetite nanoparticles from aqueous solution. The effects of adsorbent dose, pH, contact time, initial Cr(VI) concentrations, adsorption capacity, and modeling of kinetic and isotherm adsorption of Cr(VI) were investigated. Modified magnetite nanoparticles were synthesized by using a co-precipitation method, and its structural and textural properties were studied by scanning electron microscopy (SEM) and X-ray diffraction (XRD). The maximum removal of Cr(VI) was achieved at pH 4.0. A contact time of 60 min was required to reach the equilibrium. Experimental data were fitted with different nonlinear isotherm and kinetic models. The results showed that the adsorption data were fitted well by the Redlich and Peterson and Freundlich isotherm models. The kinetic data were best fitted to pseudo-second-order kinetic model. The results indicate that modified nano-sized magnetite could be employed as adsorbent for the removal of Cr(VI) in aqueous environments effectively.

Keywords: Modified magnetite nanoparticles; Chromium; Adsorption; Nonlinear modeling

1. Introduction

Water pollution by heavy metals is of considerable concern in relation to both human health and aquatic ecosystems. Although they occur naturally, the main source of heavy metals in the environment appears to

be closely related with the discharge of wastewater due to human activities [1].

Heavy metals are toxic at low concentrations and can lead to accumulation in living organisms, causing various diseases and disorders. Chromium is the among of heavy metals that cause the most concern [2] as this metal has found widespread use in electroplating, leather tanning, metal finishing, nuclear power plant, textile industries, dyeing, sugar cane production,

*Corresponding author.

chemical plants, refining ores and petroleum, produced color, and chromate preparation [3–6].

Chromium exists in two oxidation states as Cr^{3+} and Cr^{6+} [7]. The hexavalent chromium is about 500 times more toxic than the trivalent form [8]. In environmental systems, Cr(VI) exists as oxyanions such as chromate and dichromate [3,9].

Cr(VI) is known as to be carcinogenic, mutagenic, and teratogenic for the living organism and enters the human body through ingestion, inhalation or skin absorption [10,11]. The maximum contaminant levels (MCLs) for Cr^{3+} and Cr^{6+} in drinking water are 5 and 0.05 mg L^{-1} , respectively [12].

Overcoming this problem has led to the development of alternative technologies for effective Cr(VI) removal from effluents. Various physical, chemical, and biological techniques have been employed for the treatment of Cr(VI) including adsorption, ion exchange, chemical precipitation, electrolysis, reverse osmosis, and photocatalytic reduction [1,13–15].

Adsorption techniques, among others, using different activated or modified model adsorbents are the most widely employed procedures in the heavy metals treatment studies but low-cost alternatives or cost-effective adsorbents are still needed [5,16]. The nano-sized magnetite is among the most effective adsorbent to remove contaminants from the aqueous medium due to high specific surface area, high reactivity, and catalytic potential. In recent years, magnetite nanoparticles (Fe_3O_4) in the field of biological and chemical treatment such as heavy metals adsorption are considered [17,18]. Magnetite nanoparticles not only are strong adsorbent, but also active reducing. Furthermore, it is separated easily by a strong magnetic field, which is helpful in terms of recycling and reuse [9,19,20].

Physical and chemical properties of magnetite nanoparticles are strongly dependent on the size. Thus, the control and distribution of particle sizes are the challenge regardless of the particle agglomeration. Since the agglomeration reduces the specific surface area and reduction potential of nanoparticles, therefore, methods such as application of a surfactants, silica particles, polymers, zeolites, and organic ingredients have been developed to solve the agglomeration problem [3,9].

Magnetic nanoparticles can be dispersed in an aqueous solution through specific interactions between the particle surfaces and selected modifiers. Recently, modification of magnetite nanoparticles using Chitosan [2,3,7], starch [21], CaCO_3 [22], polyelectrolytes [19], the zero-valent Fe [23,24] for Cr(VI) and heavy metals adsorption has been reported. In many studies, surfactants have been used as

stabilizers and as a coating agent in the surface modification of iron oxide particles. Emulsifying properties of sodium lauryl sulfate (SLS), an anionic surfactant, lead our interest to study the feasibility of synthesizing magnetite nanoparticles modified with sodium lauryl sulfate (SLS-Mag) and to evaluate the modified magnetite nanoparticles for the removal of Cr(VI) from aqueous solutions.

2. Materials and methods

2.1. Synthesis of modified magnetite nanoparticles

The Si et al. method was modified for synthesizing SLS-Mag nanoparticles [19]. Briefly, SLS-Mag nanoparticles were synthesized using the “bottom-up” method with dropwise addition of $\text{FeCl}_2 \cdot 4\text{H}_2\text{O}$ (5.0 g L^{-1} as Fe) aqueous solution to 1.0% (w/v) SLS ($\text{NaC}_{12}\text{H}_{25}\text{SO}_4$) with continuous stirring until a homogeneous suspension of SLS-Mag was obtained. The mixture was stirred for 30 min to complete the formation of the SLS-Mag complex. Then, the pH was increased slowly to 12 by adding 0.5 M NaOH solution. The reaction mixture was subsequently aged for 1 h with constant shaking. Magnetite was prepared via controlled oxidation of a Fe^{2+} ion solution according to the following equation:



2.2. Adsorption experiments

Laboratory batch experiments were carried out to study the adsorption of Cr(VI) on SLS-Mag nanoparticles. The experiments were performed at room temperature ($20 \pm 1^\circ\text{C}$) using 150-mL Erlenmeyer flasks containing 50 mL Cr(VI) solution. Stock solution of Cr(VI) ($1,000 \text{ mg L}^{-1}$) was prepared by $\text{K}_2\text{Cr}_2\text{O}_7$, and all concentration range of Cr(VI) prepared from stock solution varied between 5 and 300 mg L^{-1} . A known amount of SLS-Mag nanoparticles was added to 50 mL of the corresponding Cr(VI) solution over a period of time on a shaker at 350 rpm. After the aqueous phase was separated magnetically, the concentration of Cr(VI) and total Cr in the solution was determined by using spectrophotometer (Dr-5,000, Hack Co.) and flame atomic absorption spectrometer (Analytic Jena, Vario 6, Germany), respectively [25]. The amount of Cr(III) was determined by subtracting the total Cr and Cr(VI).

In this study, the effect of various parameters such as pH, initial concentration of the Cr(VI), amount of adsorbent, and contact time was studied.

The adsorption of Cr(VI) by SLS-Mag nanoparticles was investigated at pH range of 2–8. The initial pH of the solution was adjusted by using 0.1 M HCl or 0.1 M NaOH. The effects of contact time (2–240 min), initial concentration of Cr(VI) (5–300 mg L⁻¹), and adsorbent dosage (0.1–3.0 g L⁻¹) were also examined throughout the experiments at 20 ± 1 °C. The amount of Cr(VI) removal was calculated from the difference between Cr(VI) taken and that remained in the solution.

The removal efficiency (R) of Cr(VI) and the adsorption capacity (q_e) were obtained by using the following equations:

$$R = \frac{C_o - C_e}{C_o} \times 100 \quad (2)$$

$$q_e = \frac{(C_o - C_e)V}{m} \quad (3)$$

where R is the removal efficiency (%), q_e the sorption capacity at equilibrium (mg g⁻¹), C_o the initial concentration of desired heavy metal (mg L⁻¹), C_e the concentration in equilibrium of desired heavy metal (mg L⁻¹), m the mass of adsorbent (g), and V volume of the solution (L).

2.3. Adsorption isotherm and kinetic models

Determination of adsorption isotherm and related parameters is a basic requirement for the design of adsorption systems. To remove contaminant such as heavy metals from water and wastewater, it is necessary to know the removal rate for the design and the quantitative evaluation of adsorbent. In addition, the kinetics describes the adsorbate uptake rate which control the residence time of adsorbate uptake at the adsorbent–solution interface. Therefore, it is important to be able to predict the metallic ion uptake removal rate from aqueous solutions in order to design an appropriate adsorption unit.

Five models, Langmuir [26], Freundlich [27], Redlich–Peterson [28], Koble–Corrigan [29], and Liu [30], were used to describe adsorption equilibrium of Cr(VI) ions by SLS-Mag nanoparticles. All the used mathematical isotherm models have been summarized in Table 1, where q is the adsorbed amount and C is the equilibrium concentration of Cr(VI), respectively. In the Langmuir model, q_m is the maximum solute adsorbed at equilibrium state for completion of a layer (mg g⁻¹) and K_L is a constant that depends on the energy of adsorption, which shows the enthalpy of adsorption and is as an index to describe the binding energy of surface adsorption. In the Freundlich model, K_F and n

are coefficients were attributed to adsorption capacity and adsorption intensity of adsorbent, respectively. K_{RP} , a_{RP} , and g in the Redlich–Peterson isotherm are model constants. K_{RP} is the solute adsorptivity (L g⁻¹), a_{RP} related to adsorption energy (L mg⁻¹) and g is the heterogeneity constant ($0 < g < 1$) [31,32]. In the Koble–Corrigan model, K_K , a_K , and α are Koble–Corrigan coefficients, which this model is valid for $\alpha > 1$. In the Liu model, K_g (L mg⁻¹) and n_L are the coefficients which are attributed to Liu equilibrium constant and exponent of the Liu equation, respectively [33].

In order to describe the kinetics of Cr(VI) adsorption onto modified magnetite nanoparticles, characteristic constants were determined using pseudo-first-order equation of Lagergren [34], pseudo-second-order equation of Ho [35], Elovich [36], and Avrami fractional order [37], which the used kinetic model expressions are also presented in Table 1. Where q_e is the Cr(VI) adsorbed at equilibrium state (mg g⁻¹), q_t is the adsorbed amount of Cr(VI) at any time t (mg g⁻¹), k_f (min⁻¹) and k_s (g mg⁻¹ min⁻¹) are the kinetic rate constants of the pseudo-first-order and pseudo-second-order, respectively, α is the initial adsorption rate (mg g⁻¹ min⁻¹), β is the adsorption constant (g mg⁻¹), k_{AV} and n_{AV} are the Avrami rate constant (min⁻¹) and fractional reaction order (Avrami), respectively.

To determine the parameters of the isotherm and kinetic models, the nonlinear method is superior to the linear one [38,39]. While the nonlinear approach is based on trial and error using “raw” experimental data to determine the model parameters, but the linear approach assumes that the data points scattered around the straight line and follow a Gaussian distribution that the distribution error is the same for each value of the abscissa. This is rarely true or almost impossible in the case of equilibrium isotherm models, because many of the isotherm models are nonlinear. Therefore, unwanted falsification of error distribution occurs due to data transformation to a linear form [39]. The Cr(VI) adsorption data were fitted to the kinetic and isotherm models using MATLAB[®] 7.11.0 (R2010b) by employing a nonlinear method, with successive interactions calculated by the Levenberg–Marquardt algorithm.

2.4. Goodness of fit model test

In this study, the goodness of fit between experimental and predicted data was assessed by the linear coefficient of determination (R^2), the adjusted determination factor (R_{adj}^2) [40], the root mean square error (RMSE), and the sum squared error (SSE) [32] as follows:

Table 1
Mathematical equations of the used isotherm and kinetic adsorption models

Model	Equation	Parameter and dimension
<i>Isotherm models</i>		
Langmuir	$q_e = \frac{K_L q_m C_e}{1 + K_L C_e}$	q_m (mg g ⁻¹) K_L (L mg ⁻¹)
Freundlich	$q_e = K_F C_e^{\frac{1}{n}}$	K_F (mg g ⁻¹) (mg L ⁻¹) ⁻ⁿ n : model exponent (-)
Redlich–Peterson	$q_e = \frac{K_{RP} C_e}{1 + a_{RP} C_e^g}$	K_{RP} (L g ⁻¹) a_{RP} (L mg ⁻¹) g (-) (0 < g < 1)
Koble–Corrigan	$q_e = \frac{K_K C_e^\alpha}{1 + a_K C_e^\alpha}$	K_K (L ⁿ mg ^{1-n/g}) a_K ((Lmg ⁻¹) ⁿ) α : model exponent (-)
Liu	$q_e = \frac{q_m (K_g C_e)^{n_L}}{1 + (K_g C_e)^{n_L}}$	K_g (L mg ⁻¹) n_L (-)
<i>Kinetic models</i>		
Pseudo-first order (Lagergren)	$q_t = q_e (1 - \exp(-k_f t))$	K_f (min ⁻¹) q_e, q_t (mg g ⁻¹)
Pseudo-second order (H _o)	$q_t = \frac{k_s q_e^2 t}{1 + q_e k_s t}$	k_s (min ⁻¹) t : time (min)
Elovich	$q_t = \left(\frac{1}{\beta}\right) \ln(\alpha\beta) + \left(\frac{1}{\beta}\right) \ln(t)$	α (mg g ⁻¹ min ⁻¹) β (g mg ⁻¹)
Avrami fractional order	$q_t = q_e \{1 - \exp[-(k_{AV} t)]^{n_{AV}}\}$	k_{AV} (min ⁻¹) n_{AV} (-)

$$R_{adj}^2 = \left\{ 1 - \left[1 - \frac{\sum_i^n (q_{i,exp} - \bar{q}_{i,exp})^2 - \sum_i^n (q_{i,exp} - q_{i,calc})^2}{\sum_i^n (q_{i,exp} - \bar{q}_{i,exp})^2} \right] \cdot \left(\frac{n-1}{n-p} \right) \right\} \quad (4)$$

$$RMSE = \sqrt{\frac{\sum_{i=1}^n (q_{i,exp} - q_{i,calc})^2}{n}} \quad (5)$$

$$SSE = \sum_{i=1}^n (q_{i,calc} - q_{i,exp})_i^2 \quad (6)$$

where $q_{i,calc}$ is each value of q predicted by the fitted model, $q_{i,exp}$ is each value of q measured experimentally, $\bar{q}_{i,exp}$ is the average of q measured experimentally, n is the number of experiments performed, and p is the number of parameters of the fitted model [32,41]. The best model is the model with the lowest RMSE and SSE, as well as with R_{adj}^2 with R^2 close to one.

2.5. Characterization of modified magnetite nanoparticles

Scanning electron microscopy (SEM) characterization was performed to identify surface morphology and size distribution of SLS-Mag nanoparticles. The functional groups presenting in SLS-Mag nanoparticles was investigated using the Fourier transform infrared (FTIR) technique. X-ray diffraction (XRD) analysis was performed to identify the structure and the composition of freshly synthesized SLS-Mag nanoparticles.

3. Results and discussion

3.1. Characterization of adsorbent

The surface and textural morphology of SLS-Mag nanoparticles by SEM image is illustrated in Fig. 1. It was found that the average particle diameter is 50 nm.

The iron oxide phase was identified from the XRD pattern, as shown in Fig. 2. Matching with standard card PDF 2 Number (01-088-0866, Fe₃O₄) showed that crystals of pure magnetite synthesized well and another phases are not available.

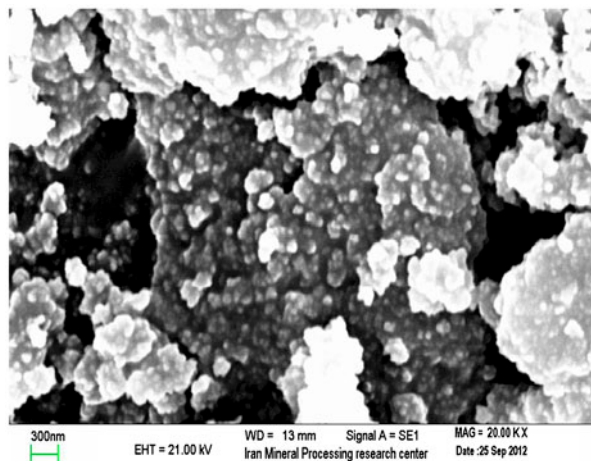


Fig. 1. SEM image of the SLS-Mag nanoparticles.

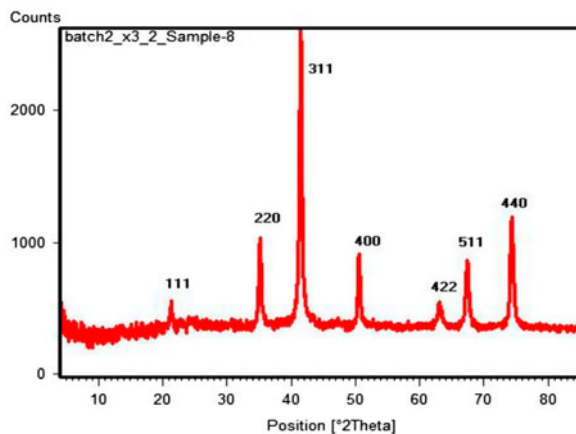


Fig. 2. XRD image of the SLS-Mag nanoparticles.

The adsorbent surface modification, namely, coating magnetite nanoparticles by SLS surfactant to prevent aggregation of magnetite nanoparticles showed a positive impact on adsorption capacity of magnetite nanoparticles. Briefly, adsorption test was conducted in the same condition with different concentration of Cr(VI), and that result showed approximately 5-fold increasing in adsorption capacity of modified magnetite nanoparticle with SLS compared to non-modified one. The nanoparticles modification with SLS leads to better dispersion of the nanoparticles and thus increase surface area for absorption of chromium and consequently, adsorption capacity would be increased. The results are strongly similar to the findings of [42]. Also, Yuan et al. reported that coated magnetite nanoparticles with silica had a better Cr(VI) adsorption capacity per mass unit compared with non-coated one due to reduction of particle agglomeration [9]. According to Zhang

et al. study, the stabilized magnetite nanoparticles with starch were more effective than the non-stabilized nanoparticles for the adsorption of arsenic [21].

3.2. Equilibrium studies

3.2.1. pH effect

Numerous studies on heavy metal adsorption have shown that pH is the single most important parameter affecting the adsorption process [43]. This study showed the maximum elimination of Cr(VI) by SLS-Mag nanoparticles was occurred at pH 4 (see Fig. 3). Results showed that a quantity of chromium (III) was formed in pH 2, but with increasing pH, the Cr(III) formation was reduced.

In many studies have been reported that the removal of Cr(VI) in acidic pH is much faster and greater than neutral and alkaline pH [3,43–45].

In this study, pH_{ZPC} of SLS-Mag nanoparticles was equal to 6.02, which the magnetite nanoparticles surface has a positive charge at pH less than pH_{ZPC} , and optimal adsorption of anionic species of Cr(VI) ($Cr_2O_7^{2-}$ and $HCrO_4^{2-}$) occurs. In contrast, at pH higher than pH_{ZPC} , SLS-Mag surface has a negative charge and the electrostatic attraction between anionic species of Cr(VI) and SLS-Mag surface decreases [3,46]. On the other hand, with increasing pH, functional groups of the adsorbent surface has a negative charge such OH^- ions that hinder the absorption of Cr(VI), and this is as a result of the repulsion between the species of Cr(VI) and SLS-Mag surface.

3.2.2. Adsorbent dose effect

The elimination of Cr(VI) was increased from 57.5 to 99.0% with increasing adsorbent dose from 0.1 to 1.0 g L^{-1} , which adsorption efficiency is almost

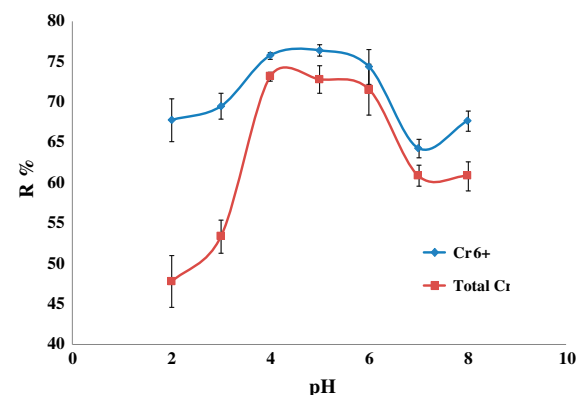


Fig. 3. Effect of pH on Cr(VI) removal by adsorption onto SLS-Mag nanoparticles. $C_o = 10\text{ mg L}^{-1}$, contact time = 120 min, adsorbent dose = 1 g L^{-1} , $T = 20 \pm 1^\circ\text{C}$.

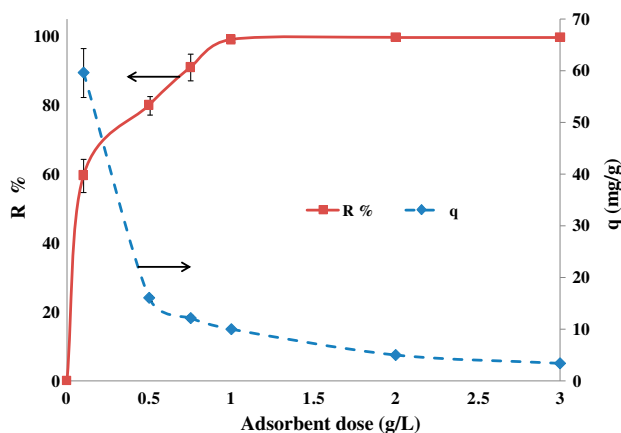


Fig. 4. Effect of adsorbent dose on Cr(VI) removal by SLS-Mag nanoparticles ($C_o = 10 \text{ mg L}^{-1}$, contact time = 120 min, $\text{pH} = 4$, $T = 20 \pm 1^\circ\text{C}$).

constant by increasing of adsorbent dose more than 1 g L^{-1} (Fig. 4). This observation can be elucidated in terms of availability of active sites on the adsorbent surface for Cr(VI) adsorption, which it is noted and expressed in the most of the studies on adsorption [43,47]. However, the removal efficiency increases with increasing adsorbent dose due to availability of active adsorption sites but the equilibrium concentration decreases. It may be concluded that the adsorption density is reduced with increasing adsorbent dose. This is due to the fact that some adsorption sites remain unsaturated for a given initial chromium concentration during the adsorption process.

3.2.3. Contact time effect

Fig. 5 represents the removal of Cr(VI) as a function of contact time using SLS-Mag. As shown, the removal efficiency increases with increasing contact time. By increasing the contact time from 2 to 60 min, the adsorption efficiency was increased from 55.9 to 99.4% and thereafter was almost constant up to the studied time of 240 min. There was no significant change in the Cr(VI) adsorption efficiency with increasing contact time over 60 min. Therefore, it is clear that adsorption of Cr(VI) into SLS-Mag is rather quick and after 1 h the complete adsorption equilibrium was obtained. Wu and Yuan et al. reported equilibrium time of 60 min for Cr(VI) adsorption from aqueous solutions by magnetite particles and montmorillonite-supported magnetite nanoparticles, respectively [3,23].

3.2.4. Adsorption kinetics

Adsorption kinetics was examined to better understand the mechanism of the adsorption process

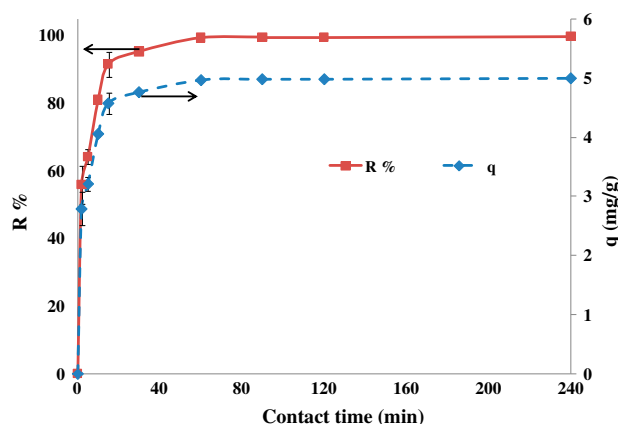


Fig. 5. Effect of contact time on adsorption of Cr(VI) ($C_o = 10 \text{ mg L}^{-1}$, $\text{pH} = 4$, adsorbent dose 2 g L^{-1} , $T = 20 \pm 1^\circ\text{C}$).

of sorbent on the adsorbent surface and to find a model to estimate the absorption rate with time, which are important in the treatment of aqueous effluents [48]. The adsorption of Cr(VI) by Mag-SLS as a function of time at initial Cr(VI) concentration of 10 mg L^{-1} and a sorbent concentration of 2 g L^{-1} are displayed in Fig. 5. The shape of the curve representing Cr(VI) uptake vs. time (Fig. 5) suggests that a two-step mechanism occurs. The first portion indicates that a rapid adsorption occurs during the first 15 min after which equilibrium is slowly achieved. More than 90% removal for Cr(VI) occurred within 15 min (Fig. 5).

In order to describe the adsorption kinetics of Cr(VI) using Mag-SLS nanoparticles, four kinetic models were tested, as shown in Fig. 6. Values of adsorption kinetic coefficients and goodness of fit parameters are calculated by the nonlinear regression analysis using MATLAB (Table 2). The R_{adj}^2 , the RMSE, and the SSE values of the different adsorption kinetic models for the selected chromium concentration (10 mg L^{-1}) suggest that pseudo-second-order model exhibits the highest correlation with experimental data indicating that the chemical reaction seems significant in the rate-controlling step. The results are similar to Abou EL-Reash et al. study on Cr adsorption by modified magnetic chitosan chelating resin [2]. According to Wang et al., Cu (II) adsorption on nano-magnetite particles best correlates with pseudo-second-order model [14].

3.2.5. Adsorption isotherms

As adsorption isotherm is an important factor in design of adsorption systems. The isotherms of adsorption were carried out with Cr(VI) on the

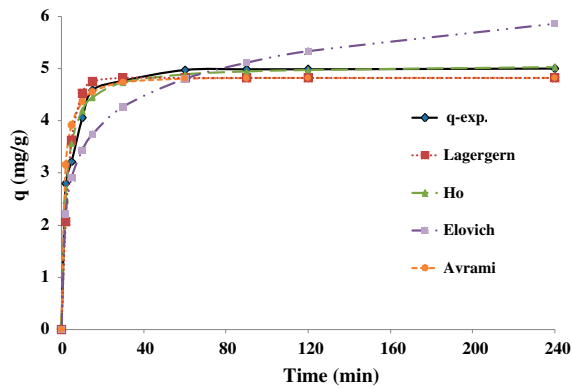


Fig. 6. Non-linear adsorption kinetics of Cr(VI) on SLS-Mag nanoparticles.

Table 2
Coefficients of adsorption kinetic models

Adsorption kinetic models	Parameters	Values
Pseudo-first order	q_e (mg g^{-1})	4.82
	K_f (min^{-1})	0.279
	RMSE	0.365
	SSE	1.065
	R_{adj}^2	0.947
Pseudo-second order	k_S ($\text{g mg}^{-1}\text{min}^{-1}$)	0.0951
	q_e (mg g^{-1})	5.064
	RMSE	0.185
	SSE	0.274
	R_{adj}^2	0.987
Elovich	α	6.87
	β	1.311
	RMSE	0.828
	SSE	5.487
	R_{adj}^2	0.73
Avrami fractional order	k_{AV} (min^{-1})	0.562
	q_e (mg g^{-1})	4.82
	n_{AV}	0.496
	RMSE	0.390
	SSE	1.065
	R_{adj}^2	0.94

SLS-Mag adsorbent and were performed using the best experimental conditions previously described (see Fig. 7). Although based on the R_{adj}^2 , RMSE, and SSE, the Koble–Corrigan (K–C) model was the best isotherm model for Cr(VI) adsorption by SLS-Mag adsorbent, but since α is less than 1, this isotherm model is invalid. Additionally, the best fit is obtained from using the Redlich–Peterson (R–P) and Freundlich models too. Regardless of the Koble–Corrigan model,

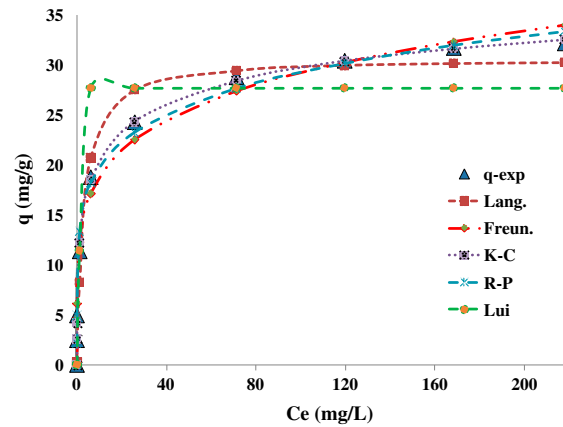


Fig. 7. Isotherm curves of Cr(VI) adsorption at $20 \pm 1^\circ\text{C}$ on SLS-Mag. (pH 4.0; adsorbent dose 2 g L^{-1} ; contact time 1 h).

the Redlich–Peterson (R–P) and Freundlich models showed (Table 3) the lowest RMSE and SSE values, which it shows the heterogeneity of the SLS-Mag nanoparticles surface. It means that the q calculated

Table 3
Isotherm parameters for chromium adsorption onto SLS-Mag

Adsorption isotherm models	Parameters	Values
Langmuir	q_m (mg g^{-1})	30.7
	K_L (L mg^{-1})	0.335
	R_{adj}^2	0.956
	RMSE	2.68
	SSE	57.63
Freundlich	K_F (L g^{-1})	10.7
	n	5.3
	R_{adj}^2	0.988
	RMSE	1.43
	SSE	16.35
Redlich–Peterson	K_{RP} (L g^{-1})	449.5
	a_{RP} (L mg^{-1})	33.33
	g (–)	0.832
	R_{adj}^2	0.993
	RMSE	1.10
	SSE	8.42
Koble–Corrigan	K_K ($\text{L}^n \text{mg}^{1-n/\text{g}}$)	12.77
	a_K ($(\text{L mg}^{-1})^n$)	0.265
	α	0.34
	R_{adj}^2	0.999
	RMSE	0.532
	SSE	1.98

Table 4
The adsorptive capacities of various adsorbents for Cr(VI)

Adsorbent	q_m (mg g^{-1})	pH	Reference
Montmorillonite-supported magnetite	11.4	2.5	[9]
Magnetite	10.6	2.5	[9]
Magnetite-maghemite	2.4	2.0	[43]
Brown coals	0.68	3.0	[52]
Coal	6.78	2.0	[53]
Carbon slurry	25.64	2.5	[54]
Activated charcoal	12.87	2.0	[55]
Coir pith carbon	120.5	2.0	[56]
CeO ₂ /ACNTs	30.3	7.0	[57]
Sulfonated lignite	27.87	2.0	[21]
SLS modified magnetite	30.7	4.0	This study

by the isotherm model (q_{calc}) was close to the q measured experimentally (q_{exp}). The Liu isotherm model was not suitably fitted, presenting higher RMSE and SSE values. Therefore, the isotherm parameters of the Liu model were not presented in Table 3.

When the constant value of the R–P equation is large enough, its form is the same as the Freundlich equation [49]. As shown in Table 3, the constant n in Freundlich model is greater than one ($n=5.3$) that indicates good adsorption conditions for Cr(VI) by SLS-Mag nanoparticles [32,50]. Other researchers have reported that heavy metals such as chromium adsorption by magnetite adsorbent followed the Freundlich isotherm model [2,14]. According to Brdar et al., Redlich–Peterson isotherm was found to be the best representative for Cr(VI) adsorption on the Kraft lignin [51].

Table 4 is presented a comparison of sorption capacities of chromium adsorbed in different adsorbents. The maximum amount of chromium uptake was 30.7 mg g^{-1} for SLS-Mag. Based on the Table 4, SLS-Mag adsorbent presented good sorption capacities compared to other adsorbents.

4. Conclusions

In this study, SLS modified magnetite (SLS-Mag) nanoparticles have been prepared via co-precipitation method and used as an effective adsorbent for the removal of chromium from aqueous solutions. The best conditions were established with respect to pH and contact time to adsorption chromium on the adsorbent surface. Four kinetic models were used to

adjust the adsorption data by employing a nonlinear method, and the best fit was the pseudo-second-order kinetic model of Ho. Five isotherm models are applied to fit the experimental data by employing a nonlinear method. The adsorption data of SLS-Mag nanoparticles fit well with the Redlich–Peterson and Freundlich isotherm models. The SLS-Mag nanoparticles exhibited good adsorption capacity per unit mass of magnetite, which found to be $30.7 \text{ mg Cr(VI) g}^{-1}$ of adsorbent. During the adsorption of Cr(VI) onto SLS-Mag nanoparticles, Cr(VI) not only can be reduced Cr(III) with less toxicity than Cr(VI) but also can be fixed into the iron oxide. These results show that the SLS-Mag nanoparticle is a robust adsorbent and readily prepared, enabling promising applications for the removal of Cr(VI) from contaminated waters with advantages such as no toxicity, simplicity, and low cost of production and ease of separation by the a magnetic field compared to other adsorbents.

Acknowledgements

This paper is issued from thesis of Zeynab Baboli. Special thanks to Vice-Chancellor for Research Affairs of Ahvaz Jundishapur University of Medical Sciences for the financial support (Grant No: ETRC9105).

References

- [1] P. Teymouri, M. Ahmadi, A.A. Babaei, K. Ahmadi, N. Jaafarzadeh, Biosorption Studies on NaCl-Modified Ceratophyllum demersum: Removal of Toxic Chromium from Aqueous Solution, Chem. Eng. Comm. 200 (2013) 1394–1413.
- [2] Y.G. Abou El-Reash, M. Otto, I.M. Kenawy, A.M. Ouf, Adsorption of Cr(VI) and As(V) ions by modified magnetic chitosan chelating resin, Int. J. Biol. Macromol. 49 (2011) 513–522.
- [3] P. Yuan, M. Fan, D. Yang, H. He, D. Liu, A. Yuan, J. Zhu, T. Chen, Montmorillonite-supported magnetite nanoparticles for the removal of hexavalent chromium [Cr(VI)] from aqueous solutions, J. Hazard. Mater. 166 (2009) 821–829.
- [4] G. Dönmez, Z. Aksu, Removal of chromium (VI) from saline wastewaters by Dunaliella species, Process Biochem. 38 (2002) 751–762.
- [5] H. Li, S. Bi, L. Liu, W. Dong, X. Wang, Separation and accumulation of Cu (II), Zn (II) and Cr (VI) from aqueous solution by magnetic chitosan modified with diethylenetriamine, Desalination 278 (2011) 397–404.
- [6] R. Ali Khan Rao, F. Rehman, M. Kashifuddin, Removal of Cr(VI) from electroplating wastewater using fruit peel of Leechi (Litchi chinensis), Desalin. Water Treat. 49 (2012) 136–146.
- [7] K.Z. Elwakeel, Removal of Cr(VI) from alkaline aqueous solutions using chemically modified magnetic chitosan resins, Desalination 250 (2010) 105–112.
- [8] Z. Kowalski, Treatment of chromic tannery wastes, J. Hazard. Mater. 37 (1994) 137–141.
- [9] P. Yuan, D. Liu, M. Fan, D. Yang, R. Zhu, F. Ge, J. Zhu, H. He, Removal of hexavalent chromium [Cr(VI)] from aqueous solutions by the diatomite-supported/unsupported magnetite nanoparticles, J. Hazard. Mater. 173 (2010) 614–621.

- [10] A. Sari, D. Mendil, M. Tuzen, M. Soylak, Biosorption of Cd (II) and Cr(III) from aqueous solution by moss (*Hylocomium splendens*) biomass: Equilibrium, kinetic and thermodynamic studies, *Chem. Eng. J.* 144 (2008) 1–9.
- [11] C.L. Warner, R.S. Addleman, A.D. Cinson, T.C. Droubay, M.H. Engelhard, M.A. Nash, W. Yantasee, M.G. Warner, High-performance, superparamagnetic, nanoparticle-based heavy metal sorbents for removal of contaminants from natural waters, *ChemSusChem* 3 (2010) 749–757.
- [12] EPA, 2011, Edition of the Drinking Water Standards and Health Advisories, in: Edition (Ed.), United States environmental protection agency, Washington, DC, 2011.
- [13] A. Sari, M. Tuzen, Biosorption of total chromium from aqueous solution by red algae (*Ceramium virgatum*): Equilibrium, kinetic and thermodynamic studies, *J. Hazard. Mater.* 160 (2008) 349–355.
- [14] X.S. Wang, L. Zhu, H.J. Lu, Surface chemical properties and adsorption of Cu (II) on nanoscale magnetite in aqueous solutions, *Desalination* 276 (2011) 154–160.
- [15] K.B. Nagashanmugam, K. Srinivasan, Removal of chromium (VI) from aqueous solution by chemically modified gingelly oil cake carbon, *Indian J. Chem. Technol.* 18 (2011) 207–219.
- [16] A. Üçer, A. Uyanik, Ş.F. Aygün, Adsorption of Cu(II), Cd(II), Zn(II), Mn(II) and Fe(III) ions by tannic acid immobilised activated carbon, *Sep. Purif. Technol.* 47 (2006) 113–118.
- [17] X.S. Wang, F. Liu, H.J. Lu, P. Zhang, H.Y. Zhou, Adsorption kinetics of Cd (II) from aqueous solution by magnetite, *Desalin. Water Treat.* 36 (2011) 203–209.
- [18] A. Zach-Maor, R. Semiat, H. Shemer, Removal of heavy metals by immobilized magnetite nano-particles, *Desalin. Water Treat.* 31 (2011) 64–70.
- [19] S. Si, A. Kotal, T.K. Mandal, S. Giri, H. Nakamura, T. Kohara, Size-controlled synthesis of magnetite nanoparticles in the presence of polyelectrolytes, *Chem. Mater.* 16 (2004) 3489–3496.
- [20] K. Babu, R. Dhamodharan, Synthesis of polymer grafted magnetite nanoparticle with the highest grafting density via controlled radical polymerization, *Nanoscale Res. Lett.* 4 (2009) 1090–1102.
- [21] M. Zhang, Y. Wang, D. Zhao, G. Pan, Immobilization of arsenic in soils by stabilized nanoscale zero-valent iron, iron sulfide (FeS), and magnetite (Fe₃O₄) particles, *Chin. Sci. Bull.* 55 (2010) 365–372.
- [22] C.S. Doyle, T. Kendelewicz, G.E. Brown, Inhibition of the reduction of Cr (VI) at the magnetite–water interface by calcium carbonate coatings, *Appl. Surf. Sci.* 230 (2004) 260–271.
- [23] Y. Wu, J. Zhang, Y. Tong, X. Xu, Chromium (VI) reduction in aqueous solutions by Fe₃O₄-stabilized Fe⁰ nanoparticles, *J. Hazard. Mater.* 172 (2009) 1640–1645.
- [24] F. dos Santos Coelho, J.D. Ardisson, F.C.C. Moura, R.M. Lago, E. Murad, J.D. Fabris, Potential application of highly reactive Fe(0)/Fe₃O₄ composites for the reduction of Cr(VI) environmental contaminants, *Chemosphere* 71 (2008) 90–96.
- [25] Annual book of ASTM standards test methods for chromium in water ASTM, American Society for Testing and Material (ASTM), Philadelphia, PA, USA, 2002.
- [26] I. Langmuir, The constitution and fundamental properties of solids and liquids. Part I. Solids, *J. Am. Chem. Soc.* 38 (1916) 2221–2295.
- [27] H.M.F. Freundlich, Over the adsorption in solution, *J. Phys. Chem.* 57 (1906) 385–470.
- [28] O. Redlich, D.L. Peterson, A useful adsorption isotherm, *J. Phys. Chem.* 63 (1959) 1024–1024.
- [29] R.A. Koble, T.E. Corrigan, Adsorption isotherms for pure hydrocarbons, *Ind. Eng. Chem.* 44 (1952) 383–387.
- [30] Y. Liu, H. Xu, S.-F. Yang, J.-H. Tay, A general model for biosorption of Cd²⁺, Cu²⁺ and Zn²⁺ by aerobic granules, *J. Biotechnol.* 102 (2003) 233–239.
- [31] X.-F. Sun, S.-G. Wang, X.-W. Liu, W.-X. Gong, N. Bao, B.-Y. Gao, Competitive biosorption of zinc(II) and cobalt(II) in single- and binary-metal systems by aerobic granules, *J. Colloid Interface Sci.* 324 (2008) 1–8.
- [32] K.Y. Foo, B.H. Hameed, Insights into the modeling of adsorption isotherm systems, *Chem. Eng. J.* 156 (2010) 2–10.
- [33] F.M. Machado, C.P. Bergmann, T.H.M. Fernandes, E.C. Lima, B. Royer, T. Calvete, S.B. Fagan, Adsorption of reactive red M-2BE dye from water solutions by multi-walled carbon nanotubes and activated carbon, *J. Hazard. Mater.* 192 (2011) 1122–1131.
- [34] S. Lagergren, About the theory of so-called adsorption of soluble substances, *Kungliga Svenska Vetenskapsakademiens, Handlingar, Band 24* (1898) 1–39.
- [35] Y.S. Ho, G. McKay, Pseudo-second-order model for sorption processes, *Process Biochem.* 34 (1999) 451–465.
- [36] M. Shirvani, H. Shariatmadari, M. Kalbasi, Kinetics of cadmium desorption from fibrous silicate clay minerals: Influence of organic ligands and aging, *Appl. Clay Sci.* 37 (2007) 175–184.
- [37] E.C.N. Lopes, F.S.C. dos Anjos, E.F.S. Vieira, A.R. Cestari, An alternative Avrami equation to evaluate kinetic parameters of the interaction of Hg(II) with thin chitosan membranes, *J. Colloid Interface Sci.* 263 (2003) 542–547.
- [38] H. Dhaouadi, F. M'Henni, Vat dye sorption onto crude dehydrated sewage sludge, *J. Hazard. Mater.* 164 (2009) 448–458.
- [39] S. Zakhama, H. Dhaouadi, F. M'Henni, Nonlinear modelisation of heavy metal removal from aqueous solution using *Ulva lactuca* algae, *Bioresource Technol.* 102 (2011) 786–796.
- [40] E.C. Lima, B. Royer, J.C.P. Vaghetti, J.L. Brasil, N.M. Simon, A.A. dos Santos Jr, F.A. Pavan, S.L.P. Dias, E.V. Benvenuti, E.A.d. Silva, Adsorption of Cu(II) on *Araucaria angustifolia* wastes: Determination of the optimal conditions by statistic design of experiments, *J. Hazard. Mater.* 140 (2007) 211–220.
- [41] D.S. Brookstein, Factors associated with textile pattern dermatitis caused by contact allergy to dyes, finishes, foams, and preservatives, *Dermatol. Clin.* 27 (2009) 309–322.
- [42] S. Wu, A. Sun, F. Zhai, J. Wang, W. Xu, Q. Zhang, A.A. Volinsky, Fe₃O₄ magnetic nanoparticles synthesis from tailings by ultrasonic chemical co-precipitation, *Mater. Lett.* 65 (2011) 1882–1884.
- [43] S.R. Chowdhury, E.K. Yanful, Arsenic and chromium removal by mixed magnetite-maghemite nanoparticles and the effect of phosphate on removal, *J. Environ. Manage.* 91 (2010) 2238–2247.
- [44] Y. Jung, J. Choi, W. Lee, Spectroscopic investigation of magnetite surface for the reduction of hexavalent chromium, *Chemosphere* 68 (2007) 1968–1975.
- [45] T.R. Santana Cadaval, A.S. Camara, G.L. Dotto, L.A.d.A. Pinto, Adsorption of Cr (VI) by chitosan with different deacetylation degrees, *Desalin. Water Treat.*, (2013) 1–10.
- [46] A. Aghakhani, S.F. Mousavi, B. Mostafazadeh-Fard, R. Rostamian, M. Seraji, Application of some combined adsorbents to remove salinity parameters from drainage water, *Desalination* 275 (2011) 217–223.
- [47] H. Hong, W.T. Jiang, X. Zhang, L. Tie, Z. Li, Adsorption of Cr (VI) on STAC-modified rectorite, *Appl. Clay Sci.* 42 (2008) 292–299.
- [48] J.C.P. Vaghetti, E.C. Lima, B. Royer, B.M. da Cunha, N.F. Cardoso, J.L. Brasil, S.L.P. Dias, Pecan nutshell as biosorbent to remove Cu(II), Mn(II) and Pb(II) from aqueous solutions, *J. Hazard. Mater.* 162 (2009) 270–280.
- [49] F.-C. Wu, B.-L. Liu, K.-T. Wu, R.-L. Tseng, A new linear form analysis of Redlich–Peterson isotherm equation for the adsorptions of dyes, *Chem. Eng. J.* 162 (2010) 21–27.
- [50] G. McKay, Adsorption of dyestuffs from aqueous solutions with activated carbon I: Equilibrium and batch contact-time studies, *J. Chem. Technol. Biotechnol.* 32 (1982) 759–772.
- [51] M. Brdar, M. Šćiban, A. Takači, T. Došenović, Comparison of two and three parameters adsorption isotherm for Cr(VI) onto Kraft lignin, *Chem. Eng. J.* 183 (2012) 108–111.

- [52] G. Arslan, E. Pehlivan, Batch removal of chromium(VI) from aqueous solution by Turkish brown coals, *Bioresource Technol.* 98 (2007) 2836–2845.
- [53] M. Dakiky, M. Khamis, A. Manassra, M. Mer'eb, Selective adsorption of chromium(VI) in industrial wastewater using low-cost abundantly available adsorbents, *Adv. Environ. Res.* 6 (2002) 533–540.
- [54] V.K. Singh, P.N. Tiwari, Removal and Recovery of Chromium (VI) from Industrial Waste Water, *J. Chem. Technol. Biotechnol.* 69 (1997) 376–382.
- [55] S. Mor, K. Ravindra, N.R. Bishnoi, Adsorption of chromium from aqueous solution by activated alumina and activated charcoal, *Bioresource Technol.* 98 (2007) 954–957.
- [56] C. Namasivayam, D. Sangeetha, Removal of chromium(VI) by ZnCl₂ activated coir pith carbon, *Toxicol. Environ. Chem.* 88 (2006) 219–233.
- [57] Z.-C. Di, J. Ding, X.-J. Peng, Y.-H. Li, Z.-K. Luan, J. Liang, Chromium adsorption by aligned carbon nanotubes supported ceria nanoparticles, *Chemosphere* 62 (2006) 861–865.